Bioorganic & Medicinal Chemistry Letters xxx (2017) xxx–xxx

Contents lists available at ScienceDirect

Bioorganic & Medicinal Chemistry Letters

journal homepage: www.elsevier.com/locate/bmcl

Design, synthesis and evaluation of 2,2-dimethyl-1,3-dioxolane derivatives as human rhinovirus 3C protease inhibitors

Qiyan Zhang [a,b], Ruiyuan Cao [b], An Liu [b], Shihai Lei [b], Yuexiang Li [b], Jingjing Yang [b], Song Li [a,b,*], Junhai Xiao [b,*]

[a] School of Pharmaceutical Engineering, Shenyang Pharmaceutical University, Shenyang 110016, Liaoning, China
[b] Laboratory of Computer-Aided Drug Design and Discovery, Beijing Institute of Pharmacology and Toxicology, Beijing 100850, China

ARTICLE INFO

Article history:
Received 13 May 2017
Revised 16 July 2017
Accepted 19 July 2017
Available online xxxx

Keywords:
HRV
3C protease inhibitors
Virtual screening
2,2-Dimethyl-1, 3-dioxolane derivatives

ABSTRACT

The human rhinovirus (HRV) is the most significant cause of the common cold all over the world. The maturation and replication of this virus entirely depend on the activity of a virus-encoded 3C protease. Due to the high conservation among different serotypes and the minimal homology existing between 3C protease and known mammalian enzymes, 3C protease has been regarded as an attractive target for the treatment of HRV infections. In this study, we identified a novel (4*R*,5*R*)-N^4-(2-((3-methoxyphenyl)amino)ethyl)-2,2-dimethyl-N^5-(naphthalen-2-yl)-1,3-dioxolane-4,5-dicarboxamide (**7a**) to be a HRV 3C protease inhibitor via virtual screening. Further research has been focused on the design, synthesis and *in vitro* biological evaluation of **7a** derivatives. The studies revealed that compound **7d** has an IC_{50} value of 2.50 ± 0.7 μM against HRV 3C protease, and it thus could serve as a promising compound for the development of novel anti-rhinoviral medicines.

The human rhinovirus (HRV) is a member of the picornavirus family and a frequent cause of the common cold.[1] Similar to other picornaviruses, HRV has a small single-stranded, positive-sense RNA genome approximately 7200 nucleotides in length,[2] which can be translated into a 220 kDa polyprotein precursor in host cells. This polyprotein precursor is proteolytically processed by two virus-encoded proteases, 2A and 3C proteases, to produce structural and functional viral components.[3] Because the generation of structural and functional viral protease is critical for viral replication, 3C protease has been regarded as an important target for the treatment of HRV infections.

Although 3C protease is a cysteine proteinase, structural analysis has revealed that it belongs to the family of chymotrypsin-like serine proteases [4]. However, unlike normal chymotrypsin-like serine proteinases, the structure of its catalytic triad is His-Glu-Cys.[5] Despite the large number of HRV serotypes (>100), 3C protease has a highly conservative cleavage site[2,6] located between glutamine (P_1) and glycine (P_1') residues[7] in the viral polyprotein substrate. Moreover, minimal homology exists between 3C protease and known mammalian enzymes,[8] making it an attractive target for the development of anti-rhinoviral drugs.

To date, the 3C protease inhibitors reported can be broadly divided into two types: peptidic and non-peptidic inhibitors (Fig. 1). Inhibitors such as Rupintrivir,[9,10] α-ketoamides,[11] peptide aldehydes,[12,13] 2-pyridone-containing peptidomimetics[14] belong to the peptidic inhibitor family, and typical non-peptidic inhibitors are heteroaromatic esters,[15] quinolone,[16] benzamides,[17,18] isatines[4] and 45240.[19] Although a large quantity of inhibitors have been discovered, none of them have been approved by the FDA for the treatment of rhinovirus infections.[15,20] Therefore, the development of effective antiviral therapies against HRV is important. Recently, many studies have focused on developing non-peptidic HRV 3C protease inhibitors owing to their smaller size and better oral bioavailability.

Herein, we report the design and synthesis of a variety of non-peptidic HRV 3C protease inhibitors bearing the scaffold of 2,2-dimethyl-1,3-dioxolane, which was generated from virtual screening. Their potencies to inhibit HRV 3C protease *in vitro* were evaluated using High Performance Liquid Chromatograph (HPLC) assay. We also explored the structure–activity relationships of 2,2-dimethyl-1,3-dioxolane derivatives with respect to inhibitory activity against HRV 3C protease.

Based on the co-crystal structure of HRV 3C protease with AG7088 [Protein Data Bank (PDB) ID: 1CQQ, 1.85 Å], we screened

* Corresponding authors at: School of Pharmaceutical Engineering, Shenyang Pharmaceutical University, Shenyang 110016, Liaoning, China (S. Li); Laboratory of Computer-Aided Drug Design and Discovery, Beijing Institute of Pharmacology and Toxicology, Beijing 100850, China (J. Xiao).

E-mail addresses: qiyanzhang1113@163.com (Q. Zhang), 21cc@163.com (R. Cao), anran1222@163.com (A. Liu), leishihai@126.com (S. Lei), ly19866528@126.com (Y. Li), yangjingjing@163.com (J. Yang), lis@bmi.ac.cn (S. Li), xiaojunhai@139.com (J. Xiao).

http://dx.doi.org/10.1016/j.bmcl.2017.07.049
0960-894X/

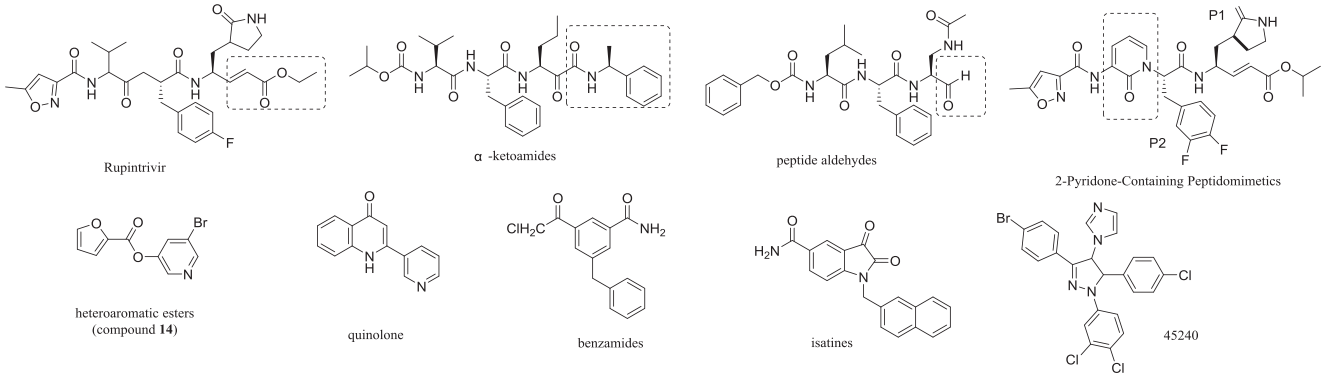

Fig. 1. HRV 3C protease inhibitors.

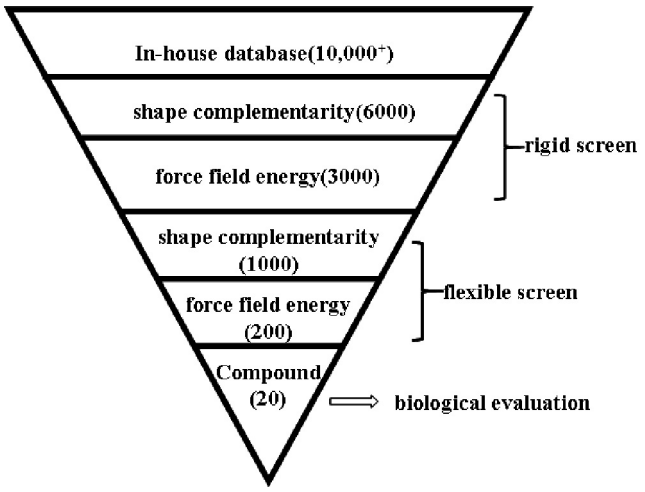

Fig. 2. The process of virtual screening from our in-house database using DOCK 6.0.

our in-house database using DOCK 6.0, which included nearly 10,000 small organic compounds. Following four rounds of rigid and flexible virtual screens, the 200 molecules with the best shape complementarity scores and force field scores were selected from the DOCK 6.0 screening. The resulting 20 compounds, which occupied the S1, S1′and S2 pockets of HRV 3C protease and formed several H-bonds with critical His40, Glu71, Gly145 and Cys147, were then chosen for the biological evaluation. The process of the virtual screening are shown in Fig. 2.

The HRV 3C protease inhibitory evaluation was performed using a High Performance Liquid Chromatograph (HPLC) assay. Compound **14**[15] was selected as a positive control, with an IC_{50} value of 0.4 ± 0.06 μM in the biological evaluation system. The structure of compound **14** is shown in Fig. 1. The HRV 3C protease inhibitory evaluation is given in Supplementary information.

The resulting 20 compounds were tested at a concentration of 100 μM. Among them, the most active compound **7a** (80.56% inhibition at 100 μM), which is novel to inhibit HRV 3C protease, was selected as a starting structure in this work for further optimization. The docking models for **7a** in the active sites are shown in Fig. 3.

The docking results suggest that there were several key interactions between **7a** and HRV 3C protease in the S1′, S1 and S2 pockets (Fig. 3). Six H-bonds were observed in the binding mode, among which two key H-bonds were formed between the oxygen of the 1,3-dioxolane ring and the catalytic His40 (2.1 Å) and Gly145 (2.1 Å) respectively. Additionally, one H-bond was formed by the hydrogen of the amide group on the C_4 atom with Val162 (2.7 Å) in the S2 pocket, and another critical H-bond was formed by the NH of the diamine group with Gly164 (2.3 Å) in the S1 pocket. Moreover, the 2-naphthalene ring and the residues in the S2 pocket can interact through hydrophobic interaction.

The above observations indicated that increased potency might be achieved by the introduction of proper substituents at C_4/C_5 position of the (*R*,*R*)-2,2-dimethyl-1,3-dioxolane, which was considers as a core structure. Considering Gly164 in the S1 pocket could form H-bond with the NH in diamine substituent, a series of piperazine substituents were designed. Due to the S2 pocket could accommodate large hydrophobic ligands, a series of aromatic

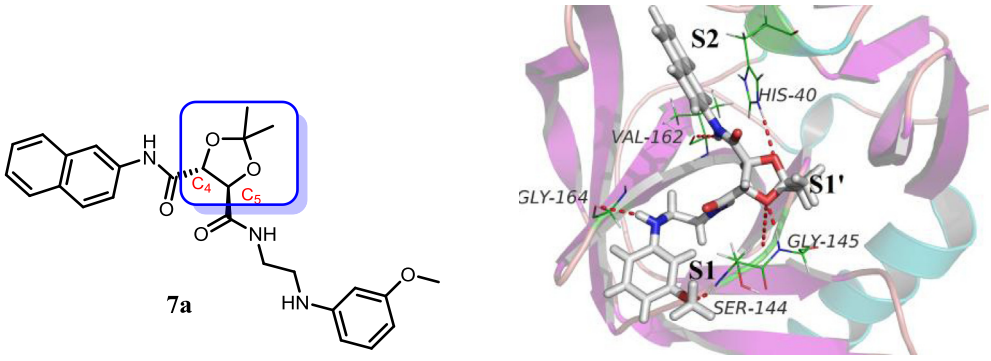

(a) (b)

Fig. 3. (a) Structures of compound **7a**, (b) Structure of compound **7a** docked in the active site with important H-bonds shown by red lines.

Table 1
% Inhibition and IC_{50} values of compounds **7a**–**7g** tested against HRV 3C protease.

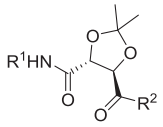

7a-7g

Compd	R^1	R^2	% inhibition at 100 μM	% inhibition at 10 μM	IC_{50} (μM)
7a	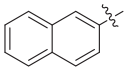	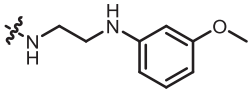	80.56	43.99	>10
7b	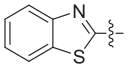	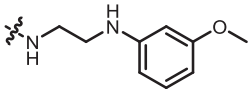	99.91	62.24	8.28 ± 1.94
7c	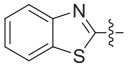	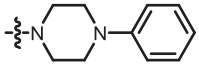	100.00	68.98	8.57 ± 1.09
7d	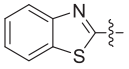	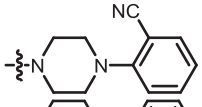	100.00	86.05	2.50 ± 0.7
7e	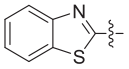	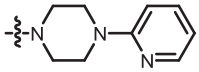	97.80	64.41	10.62 ± 2.63
7f	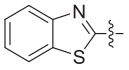	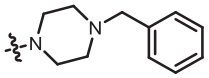	85.51	18.78	>10
7g	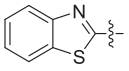	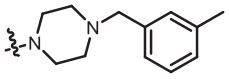	78.74	20.22	>10

substituents were designed to improve potency. To explore the relationship between compounds configuration and inhibitory activities, a series of (*S*,*S*)-2,2-dimethyl-1,3-dioxolane derivatives were designed.

The structures of designed compounds are shown in Tables 1 and 2. They were synthesized following the route shown in Schemes 1 and 2. As shown in Scheme 1, the (*R*,*R*)-2,2-dimethyl-1,3-dioxolane derivatives **7a**–**7g** were prepared in five steps. Starting from commercially available D-(+)diethyl tartrate (**1**), 2,2-dimethoxypropane (**2**) and *p*-toluenesulfonic acid, (*R*,*R*)-2,2-dimethyl-1,3-dioxolane **3** was yielded.[21] Ehrlich reagent was chosen to monitor the reaction instead of TLC analysis due to the poor UV absorption of the starting materials. After the hydrolysis of the diethyl compound **3** with NaOH, the resulting monomethyl ester **4** was then treated with 1*H*-benzo[*d*][1,2,3]triazol-1-ol(HOBt), dicyclohexylcarbodiimide (DCC) and various amines to give amide **5**, which was converted to formic acid **6** by treatment with NaOH. The condensation of **6** was performed with various amines in the presence of HOBt and DCC to give the desired (*R*,*R*)-2,2-dimethyl-1,3-dioxolane derivatives **7a**–**7g**. As shown in Scheme 2, the (*S*,*S*)-2,2-dimethyl-1,3-dioxolane derivatives **13b**–**13g** were prepared in the same methods. All the compounds and intermediates were confirmed by ^1H, ^{13}C NMR and Mass spectral data. The characterization data of all the compounds are given in Supplementary information.

In order to determine the configuration of the target compounds, amide **11a** were synthesized according to Scheme 2. The compounds **5a** and **11a** could be completely separated by reverse-phase HPLC (Agilent, Chiralpak (4.6 × 250 mm, 5 μm) with a isocratic of 50 mM KH_2PO_4 (40%, v/v) and methanol (60%, v/v) for 80 min. The peaks were monitored at 220 nm. HPLC spectrum of compounds **5a** or **11a** only contains a single peak. These show that the target compounds did not undergo configuration changes. The HPLC spectrum of compound **5a** and **11a** are given in Supplementary information.

All synthesized target compounds **7a**–**7g** and **13b**–**13g** were tested for HRV 3C protease inhibitory activity, with the data presented in Tables 1 and 2. Compared with compound **7a** (inhibitory activity <50% at 10 μM), compounds **7b** (IC_{50} = 8.28 ± 1.94 μM) showed significantly improved in potencies. Docking result of **7b** (Fig. 4a) suggested the benzothiazole ring could position well in the S2 pocket and form hydrophobic interaction. Meanwhile, the thiazole ring was observed to form π-stacking interaction with His40. Therefore, compounds **7b**–**7g**, which have benzothiazolamine substitutions, were designed, synthesized and evaluated. The inhibitory activities of compounds **7b**–**7e** (IC_{50}s at μM level) revealed that a aromatic ring with various substituents seemed to contribute less to the potency. To explore the binding modes of the R^2 substitutions, one of the most active inhibitors (**7d**) was selected as a representative and docked to the crystal structure of HRV 3C protease (PDB: 1CQQ). The docking results suggest that there were several key interactions between **7d** and HRV 3C protease in the S1, S1′ and S2 pockets. Five H-bonds were observed in the binding mode, as shown in Fig. 4b, among which two key H-bonds were formed between the oxygen of the 1,3-dioxolane ring and the catalytic His40 (2.3 Å) and Gly145 (2.9 Å), respectively. Additionally, one H-bond was formed by the NH of the amide group on the C_4 atom with Val162 (1.8 Å) in the S2 pocket, and another critical H-bond was formed by the O of the amide group on the C_5 with Gly164 (2.7 Å) in the S1 pocket. Moreover, the thiazole ring was observed to form π-stacking interaction with His40, which might be resulted in the dramatic inhibitory activity

Table 2
% Inhibition and IC_{50} values of compounds **13b**–**13g** tested against HRV 3C protease.

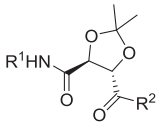

Compd	R^1	R^2	% inhibition at 100 μM	% inhibition at 10 μM	IC_{50} (μM)
13b	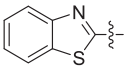	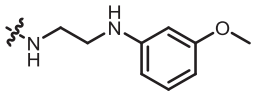	85.22	43.61	>10
13c	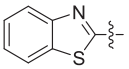	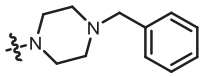	67.80	17.51	>10
13d	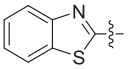	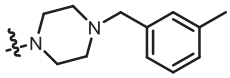	84.20	48.11	>10
13e	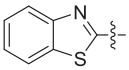	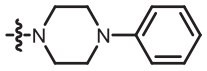	82.47	10.77	>10
13f	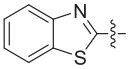	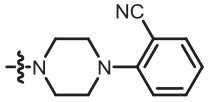	56.36	20.75	>10
13g	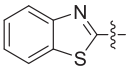	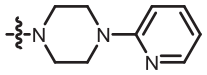	85.35	34.30	>10

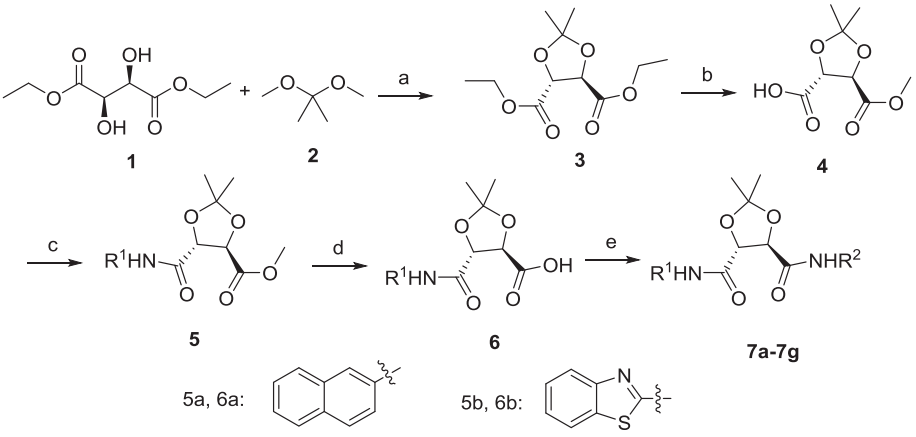

Scheme 1. Reagents and conditions: a) $CHCl_3$, *p*-toluenesulfonic acid, reflux 17 h, 42.8%, b) KOH, CH_3OH, rt, 24 h, 95.0%, c) HOBt, DCC, THF, rt, 12 h, 62.5–95%, d) H_2O/dioxane (1:1), NaOH dropped, rt, 2 h, 84.4–95.0%, e) HOBt, DCC, THF, rt, 2 h, 8.6–66.7%.

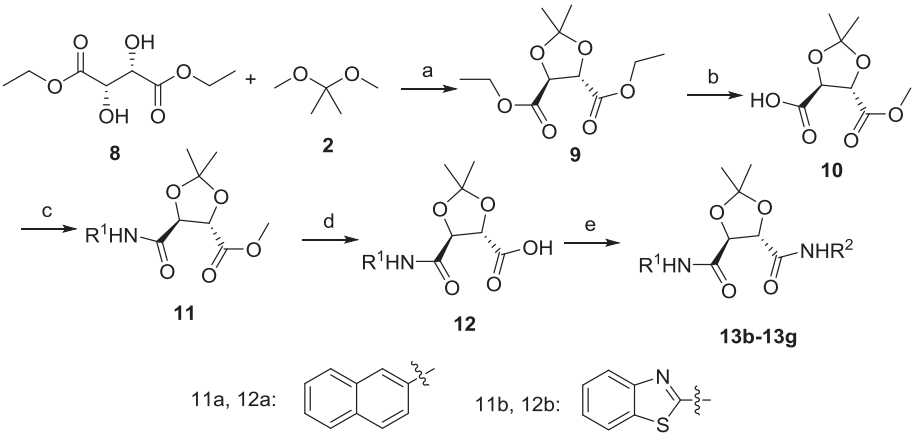

Scheme 2. Reagents and conditions: a) $CHCl_3$, *p*-toluenesulfonic acid, reflux 17 h, 42.8%, b) KOH, CH_3OH, rt, 24 h, 95.0%, c) HOBt, DCC, THF, rt, 12 h, 70.0–95.5%, d) H_2O/dioxane (1:1), NaOH dropped, rt, 2 h, 91.2%, e) HOBt, DCC, THF, rt, 2 h, 8.6–66.7%.

Please cite this article in press as: Zhang Q., et al. Bioorg. Med. Chem. Lett. (2017), http://dx.doi.org/10.1016/j.bmcl.2017.07.049

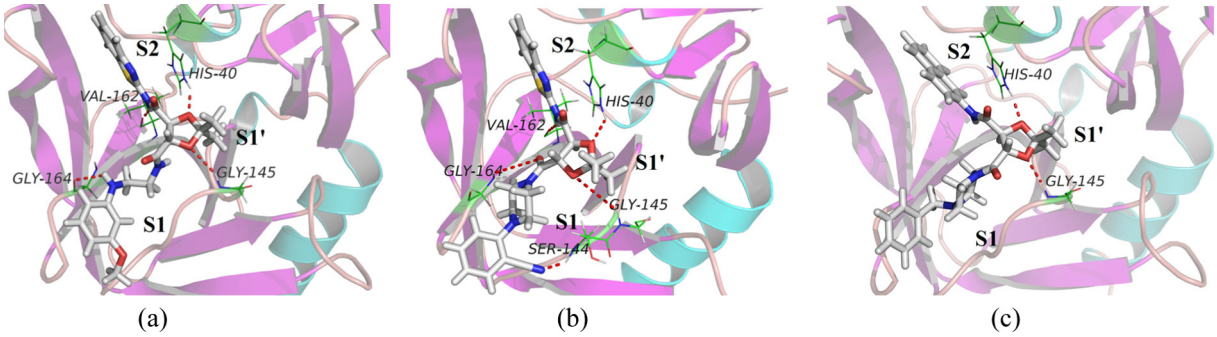

Fig. 4. (a) Structure of compound **7b** docked in the active site with important H-bonds shown by red lines. (b) Structure of compound **7d** docked in the active site with important H-bonds shown by red lines. (c) Structure of compound **7f** docked in the active site with important H-bonds shown by red lines.

changes depending on the substituents R^1. Just as expected, the benzothiazole ring and the residues in the S2 pocket can interact through hydrophobic interaction.

Compared with compound **7b**–**7e** (IC_{50}s at μM level), compounds **7f** and **7g** (inhibitory activity <50% at 10 μM) exhibited poor inhibitory activities. To explain the poor activities, compound (**7f**) was selected as a representative and docked to the crystal structure of HRV 3C protease (PDB: 1CQQ). Docking result of compound **7f** (Fig. 4c) suggested the 1-benzylpiperazine substitution could not position well in the S1 pocket and fewer H-bonds were observed. Thus, increasing the number of C atoms at the R^2 substituents will reduce the inhibitory activities.

Compared with compound **7b**–**7g**, compounds **13b**–**13g** (inhibitory activity <50% at 10 μM) showed lower inhibitory activities. This result indicates that the activity varies significantly depending on the compound configuration. Moreover, (*R*,*R*)-2,2-dimethyl-1,3-dioxolane derivatives exhibited better inhibitory activities.

In conclusion, a computer-based database screening strategy was employed to identify a novel series of 2,2-dimethyl-1,3-dioxolane derivatives as ligands for the HRV 3C protease pocket. Moreover, thirteen 2,2-dimethyl-1,3-dioxolane derivatives were designed, synthesized and evaluated as HRV 3C protease inhibitors in an enzymatic assay. Four compounds (**7b**, **7c**, **7d**,**7e**) were found to have IC_{50}s at μM level, especially compound **7d** (IC_{50} = 2.50 ± 0.7 μM) which exhibited promising inhibitory activity against HRV 3C protease. This study provides new light for further research on 3C protease inhibitors and a new strategy for the design of new anti-rhinoviral drugs.

Acknowledgments

This work was supported by the National Science and Technology Major Project of China (2014zx09304-001), the National Science Foundation for Distinguished Young Scholars of China to Dr. Cao (81302702) and State Key Laboratory of Toxicology and Medical Countermeasures (Academy of Military Medical Sciences).

A. Supplementary data

Supplementary data associated with this article can be found, in the online version, at http://dx.doi.org/10.1016/j.bmcl.2017.07.049.

References

1. Xian M, Wang QM, Chen X, et al. *Bioorg Med Chem Lett*. 2000;10:2097.
2. Jeong JY, Sperry J, Taylor JA, et al. *Eur J Med Chem*. 2014;87:220.
3. Singh SB, Graham PL, Reamer RA, et al. *Bioorg Med Chem Lett*. 2001;11:3143.
4. Webber SE, Tikhe J, Worland ST, et al. *J Med Chem*. 1996;39:5072.
5. Matthews DA, Dragovich PS, Webber SE, et al. *Proc Natl Acad Sci USA*. 1999;96:11000.
6. Steindl T, Laggner C, Langer T. *J Chem Inf Model*. 2005;45:716.
7. Reich SH, Johnson T, Wallace MB, et al. *J Med Chem*. 2000;43:1670.
8. Maugeri C, Alisi MA, Apicella C, et al. *Bioorg Med Chem*. 2008;16:3091.
9. Binford SL, Weady PT, Maldonado F, et al. *Antimicrob. Agents. Ch.*. 2007;51:4366.
10. Patick AK, Binford SL, Brothers MA, et al. *Antimicrob. Agents. Ch.*. 1999;43:2444.
11. Chen SH, Lamar J, Victor F, et al. *Bioorg Med Chem Lett*. 2003;13:3531.
12. Webber SE, Okano K, Little TL, et al. *J Med Chem*. 1998;41:2786.
13. Shepherd TA, Cox GA, McKinney E, et al. *Bioorg Med Chem Lett*. 1996;6:2893.
14. Dragovich PS, Prins TJ, Zhou R, et al. *J Med Chem*. 2002;45:1607.
15. Im I, Lee ES, Choi SJ, et al. *Bioorg Med Chem Lett*. 2009;19:3632.
16. Baxter A, Chambers M, Edfeldt F, et al. *Bioorg Med Chem Lett*. 2011;21:777.
17. Maugeri C, Alisi MA, Apicella C, et al. *Bioorg Med Chem*. 2008;16:3091.
18. Wang HM, Liang PH. *Expert Opin Ther Pat*. 2010;20:59.
19. Kuo CJ, Liu HG, Lo YK, et al. *FEBS Lett*. 2009;583:549.
20. Baxter A, Chambers M, Edfeldt F, et al. *Bioorg Med Chem Lett*. 2011;21:777.
21. Khan SW, Zaidi JH, Khan GS, et al. *J Iran Chem Soc*. 2015;12:1819.